UCSF
UC San Francisco Previously Published Works

Title

Alpha-7 nicotinic acetylcholine receptor agonist treatment reduces neuroinflammation, oxidative stress, and brain injury in mice with ischemic stroke and bone fracture

Permalink

https://escholarship.org/uc/item/4zf032v6

Journal

Journal of Neurochemistry, 131(4)

ISSN

0022-3042

Authors

Han, Zhenying
Li, Li
Wang, Liang
et al.

Publication Date

2014-11-01

DOI

10.1111/jnc.12817

Peer reviewed

eScholarship.org Powered by the California Digital Library
University of California

NIH Public Access
Author Manuscript
J Neurochem. Author manuscript; available in PMC 2015 November 01.

Published in final edited form as:
J Neurochem. 2014 November ; 131(4): 498–508. doi:10.1111/jnc.12817.

Alpha-7 nicotinic acetylcholine receptor agonist treatment reduces neuroinflammation, oxidative stress and brain injury in mice with ischemic stroke and bone fracture

Zhenying Han[1,2], **Li Li**[1], **Liang Wang**[1], **Vincent Degos**[1,3], **Mervyn Maze**[1], and **Hua Su**[1]

[1]Center for Cerebrovascular Research, Department of Anesthesia and Perioperative Care, University of California, San Francisco, San Francisco, California, USA

[2]Department of Neurosurgery, Tianjin Medical University General Hospital, Tianjin, China

[3]INSERM, U676, Hôpital Robert Debré, Paris, France

Abstract

Bone fracture at the acute stage of stroke exacerbates stroke injury by increasing neuroinflammation. We hypothesize that activation of α-7 nicotinic acetylcholine (α-7 nAchR) agonist attenuates neuroinflammation and oxidative stress, and reduces brain injury in mice with bone fracture and stroke. Permanent middle cerebral artery occlusion (pMCAO) was performed in C57BL/6J mice followed by tibia fracture 1 day later. Mice were treated with 0.8 mg/kg PHA568487 (PHA, α-7 nAchR-specific agonist), 6 mg/kg Methyllycaconitine (MLA, α-7 nAchR antagonist), or saline 1 and 2 days after pMCAO. Behavior was tested 3 days after pMCAO. Neuronal injury, $CD68^+$, M1 (pro-inflammatory) and M2 (anti-inflammatory) microglia/macrophages, phosphorylated p65 component of NF-kb in microglia/macrophages, oxidative and anti-oxidant gene expression were quantified. Compared to saline-treated mice, PHA-treated mice performed better in behavioral tests, had fewer apoptotic neurons ($NeuN^+TUNEL^+$), fewer $CD68^+$ and M1 macrophages, and more M2 macrophages. PHA increased anti-oxidant gene expression and decreased oxidative stress and phosphorylation of NF-κb p65. MLA had the opposite effects. Our data indicate that α-7 nAchR agonist treatment reduces neuroinflammation and oxidative stress, which are associated with reduced brain injury in mice with ischemic stroke plus tibia fracture.

Keywords

macrophage polarization; middle cerebral artery occlusion; neuroinflammation; oxidative stress

Introduction

Stroke is the fourth leading cause of death in the United States (Go *et al.* 2013) and an important risk factor for bone fracture (Kanis *et al.* 2001). About 70,000 people experience a

Address correspondence to: Hua Su, MD, University of California, San Francisco, Dept of Anesthesia and Perioperative Care, 1001 Potrero Avenue, Box 1363, San Francisco, CA 94110, Phone: 415-206-3162, Fax: 415-206-8907, hua.su@ucsf.edu.

Conflict-of-interest disclosure: The authors have no conflicts of interest to declare.

NIH-PA Author Manuscript
NIH-PA Author Manuscript
NIH-PA Author Manuscript

NIH-PA Author Manuscript

NIH-PA Author Manuscript

NIH-PA Author Manuscript

fracture within the first year, and in the United States about 1-1.5% of fractures occur within the first 24 hours of stroke (Kanis *et al.* 2001). We have shown that bone fracture one day after ischemic stroke in mice exacerbates neuronal injury and behavioral deficits, which were associated with an increase of microglia/macrophage infiltration in the peri-infarct region (Degos *et al.* 2013).

Inflammation after stroke can be beneficial. However, excessive inflammation during the acute phase can incur further damage (Hayakawa *et al.* 2010); conversely, reducing inflammation during the acute phase of ischemic stroke decreases brain injury and improves functional outcome (Hayakawa *et al.* 2010). In addition, microglia and macrophages mobilize to the injury site following stroke (Schroeter *et al.* 1994), and can polarize into type I (pro-inflammation, M1) and type II (anti-inflammation, M2) (Hu *et al.* 2012; Kigerl *et al.* 2009; Durafourt *et al.* 2012). Reduction of M1 and increase of M2 macrophages may reduce neuronal injury and improve functional recovery.

Oxidative stress has been implicated in the pathogenesis of brain injuries during ischemic or hemorrhagic stroke (Paravicini and Sobey 2003; Klein and Ackerman 2003) through processes that involve nicotinamide adenine dinucleotide phosphate (NADPH) oxidase (Wang *et al.* 2013). Upregulation of NADPH oxidase after brain injury triggers neuroinflammation and increases proinflammatory factors (Chen *et al.* 2011). NADPH oxidase is regulated by the inflammatory transcription factor, nuclear factor kappa b (NF-κb) (Anrather *et al.* 2006).

While cigarette smoking is considered a risk factor for ischemic stroke (Hawkins *et al.* 2002; Fujii *et al.* 2013; Naik *et al.* 2014; Mazzone *et al.* 2010; Raval *et al.* 2013), some animal studies have shown that nicotine has a beneficial effect on stroke recovery (Gonzalez *et al.* 2006; Yang *et al.* 2008). Alpha-7 nicotinic acetylcholine receptor (α-7 nAchR) is ubiquitously expressed in the brain (Quik *et al.* 2009; Breese *et al.* 1997; Woodruff *et al.* 2011). In a rat subarachnoid hemorrhage model (Duris *et al.* 2011) and in a mouse intracerebral hemorrhage model (Krafft *et al.* 2012), activation of α-7 nAchR reduced brain injury. Potentiating α-7 nAchR using type-II positive allosteric modulator also reduces brain injury and improves neurological function after transient focal cerebral ischemia in rats (Sun *et al.* 2013). More importantly, α-7 nAchR expressed on the surface of macrophages is a pivotal regulator of NF-κb activity (Wang *et al.* 2003; Tracey 2009). Treatment of bone marrow-derived macrophages with an α-7 nAchR-specific agonist, PHA 568487, prevented NF-κb activation in the cells (Terrando *et al.* 2011). Terrando et al. showed that PHA 568487 treatment reduces mouse cognitive decline caused by aseptic bone fracture by promoting inflammation resolution (Terrando *et al.* 2011).

Previous studies attribute the neuroprotection of α-7 nAchR to its pro-survival effect (Duris *et al.* 2011; Krafft *et al.* 2012). In this study using mice with stroke and tibia fracture, we tested the hypothesis that inhibition of neuroinflammation and oxidative stress are also underlying mechanisms of α-7 nAchR neuroprotection.

NIH-PA Author Manuscript

NIH-PA Author Manuscript

NIH-PA Author Manuscript

Methods

Animals

Animal experimental procedures were approved by the Institutional Animal Care and Use Committee at the University of California, San Francisco, and conformed to National Institutes of Health guidelines. Mice were fed standard rodent food and water ad libitum, and were housed (5 per cage) in sawdust-lined cages in an air-conditioned environment with 12-hour light/dark cycles.

C57BL/6J male mice (10-12 weeks old; Jackson Laboratory, Bar Harbor, ME) were randomly assigned to each treatment group. Fig. 1 shows the experimental design. Researchers blinded to the group assignment performed neurobehavioral tests, infarct volume assessment, and cell counting.

Permanent middle cerebral artery occlusion (pMCAO) procedure

Mice were anesthetized with 2% isoflurane inhalation. A 1-cm skin lesion from the left orbit to the ear was made, followed by a 2 mm^2 craniotomy under aseptic surgical conditions. The middle cerebral artery (MCA) was then permanently occluded (pMCAO) using electrical coagulation just proximal to the pyriform branch (Degos *et al.* 2013). The rectal temperature was maintained at 37 ± 0.5°C using a thermal blanket during surgery. A laser Doppler flow-meter (Vasamedics, Little Canada, MN) was used to monitor the surface cerebral blood flow to ensure the success of MCA occlusion. Mice with surface cerebral blood flow in the ischemic core >15% of the baseline, or had massive bleeding due to the artery injuries, were excluded from experiments. In this study, 7 mice were euthanized due to massive arterial bleeding during the pMCAO procedure, and were replaced with additional mice housed in the same cages. Two doses of buprenorphine (0.1 mg/kg of body weight) were injected intraperitoneally at the beginning of the surgery and 4 hours after. Mice were allowed to recover spontaneously under warm conditions.

Tibia fracture procedure

One day after the pMCAO procedure, animals were anesthetized with 2% isoflurane inhalation. Under aseptic surgical conditions, animals received an open tibia fracture on the right hind limb with an intramedullary fixation, as previously described (Cibelli *et al.* 2010). Animals were allowed to recover spontaneously from anesthesia under warm conditions. Rectal temperature was maintained at 37±0.5°C using a thermal blanket throughout the surgical procedure. Two doses of buprenorphine (0.1 mg/kg of body weight) were injected intraperitoneally at the beginning of the surgery and 4 hours after. The tibia fracture surgery did not cause any mortality.

Chemical reagents

PHA 568487 (PHA, Tocris Bioscience), a selective agonist of α-7 nAchR, and methyllycaconitine (MLA, Sigma), an antagonist of α-7 nAchR, were diluted in 0.9% saline prior to use and injected at the time indicated in Fig. 1. Using pMCAO mice, we performed a dose-response study in which PHA (0.4 and 0.8 mg/kg) or MLA (4mg and 6 mg/kg) were injected into the mice (a) once on day 1, or (b) twice on days 1 and 2, after pMCAO. The

NIH-PA Author Manuscript

NIH-PA Author Manuscript

NIH-PA Author Manuscript

testing doses were selected based on previous studies (Terrando *et al.* 2011; Duris *et al.* 2011). We found that injection of PHA (0.8 mg/kg) and MLA (6 mg/kg) on days 1 and 2 after pMCAO yielded the best effect on infarct volume and behavior tests. Therefore, 0.8 mg/kg for PHA and 6 mg/kg for MLA were used in this study.

Behavioral tests

Adhesive removal test was performed to assess potential somatosensory neglect (Bouet *et al.* 2007). Briefly, a piece of adhesive tape (0.3 × 0.3 cm) was placed on one of the forepaws. The time it took for the mouse to remove the tape was recorded. The maximum testing time was 120 seconds. Mice were trained twice daily for 4 days before pMCAO to obtain an optimal level of performance. The adhesive removal times were recorded after 2 practice trials 1 day before pMCAO (D1), and 3 days after (D3). Since the infarct in our model was on the left side of the brain, the adhesive removal times from the right paw were more relevant and are thus reported here.

Corner test was performed to detect sensorimotor and postural asymmetries after ischemic stroke (Zhang *et al.* 2002). Mice were placed between two 30 × 20 cm boards. Both sides of their vibrissae were stimulated as they approached the corner. The mice would then move up and turn to face the open end. For normal mice, the frequency of right and left turns was the same, whereas the stroke mice turned more to the ipsilateral side of the lesion (to the left in this study). Three different sets of 10 trials were conducted. Turning not incorporated in a rearing movement was excluded.

Infarct volume estimation

Both triphenylterazolum chloride (TTC) and cresyl violet staining are routinely used to determine infarct volume (Tureyen *et al.* 2004). We chose crysyl violet staining because the adjacent sections could be used for other histological analyses, thus saving on animal usage (the TTC method would have required using all brain tissues). Three days after pMCAO, mice were perfused with 4% paraformaldehyde (PFA) and brain samples were then collected. A series of 20-μm-thick coronal sections were made, of which 1 in 10 (200 μm apart) was stained with cresyl violet, imaged, and digitalized using Image J (National Institutes of Health, Bethesda, MD). The infarct areas were outlined and their pixel areas quantified. The infarct volumes were estimated by multiplying the sum of infarct areas from all cresyl violet-stained sections by 200 μm.

Cytokine level quantification

Brain samples were collected after being perfused with saline to prevent blood contamination. The cortex that contained the infarct and peri-infarct regions, from bregma 1.7 mm to -2.1 mm (about 8 mm^3), was harvested under a dissection microscope and placed in RNAlater™ solution (Qiagen, Valencia, CA). RNA was then extracted using Trizol Reagent (Qiagen), and reverse-transcribed using High Capacity RNA to cDNA kit (Applied Biosystems, Carlsbad, CA). TaqMan Fast Advanced Master Mix and gene-specific primers and probes from Applied Biosystems, including GAPDH (Mm99999915_g1), CD11b (Mm00434455_m1), iNOS (Mm00440502_m1), CD206 (Mm00485148_m1), SOD1 (Mm01344233_g1), GPX1 (Mm00656767_g1), gp91phox (Mm01287743_m1) and

NIH-PA Author Manuscript

NIH-PA Author Manuscript

NIH-PA Author Manuscript

p22phox (Mm00514478_m1), were used. Samples were run in triplicate. Specific gene expression was normalized to GAPDH and calculated using the comparative threshold cycle (ΔCT). Results were presented as fold-changes relative to the mean value of saline-treated pMCAO+tibia fracture mice.

Histological analysis

Three sections (200 μm apart) from each brain (selected from the same sets of serial sections used for infarct volume analysis) were used for each immunostaining as indicated below. Sections were incubated at 4°C overnight with the following primary antibodies: CD68 (to detect active microglia/macrophages; 1:50, AbD Serotec, Raleigh, NC), NeuN (to label neuron; 1:500, Millipore, Bedford, MA), Iba-1 (to label total microglia/macrophages; 1:200, Wako, Richmond, VA), CD11b (to identify M1 cells; 1:200, AbD Serotec, Raleigh, NC), CD206 (to identify M2 cells; 1:100, R&D, Minneapolis, MN), and NF-κb (to measure the activity of NF-κb inflammatory pathway; 1:100, Cell Signaling, Danvers, MA). After washing with phosphate-buffered saline (PBS), sections were then incubated with secondary antibodies: Alexa-594 or Alexa-488 IgG (1:500, Invitrogen, Carlsbad, CA). Negative controls were performed by omitting the primary or the secondary antibodies during the staining procedure.

Terminal deoxynucleotidyl transferase-mediated dUTPnick end-labeling (TUNEL) assay was performed using ApopTag (Millipore, Bedford, MA). Positively stained cells were counted using Image J by 3 researchers who were blinded to the research groups.

Statistical analysis

Data are presented as mean ± standard deviation (SD). Gaussian distribution was tested with d'Agostino and Pearson omnibus normality test. Equality of variances was tested with the F-test. For comparisons of more than two groups, means were compared using one-way analysis of variance (ANOVA) followed by t-tests with a Bonferroni-corrected alpha level.

Based on previous behavior data (Degos *et al.* 2013), we estimated that a sample of 9 mice per group was sufficient to demonstrate a decrease of 10 seconds to remove the adhesive in the right paw (40 vs 30 seconds with a SD of 6 seconds for each group), with 80% power at the 0.016 alpha level (after adjusting for 3 comparisons) to reach a significant difference. Thus, we used 11 mice per group for behavioral tests. The baseline behavior data presented in Fig. 2 are a combination of data obtained from mice that were subjected to pMCAO only and pMCAO+tibia. Brain samples were collected after behavioral tests on day 3 after pMCAO; 7 were used for quantification of infarct volume, apoptotic neurons, microglia/macrophages (total, M1 and M2) on histological stained sections; and 4 were used for analysis of cytokine using real-time RT-PCR.

A p value of < 0.05 was considered statistically significant for 2-group comparisons and the significant threshold was adjusted for multiple comparisons with a Bonferroni correction. Prism 6 (GraphPad Software Inc, La Jolla, CA) was used to conduct the statistical analysis.

NIH-PA Author Manuscript

NIH-PA Author Manuscript

NIH-PA Author Manuscript

Results

α-7 nAchR agonist treatment reduced behavioral deficits

Mice subjected to pMCAO alone had impaired ability to remove the adhesive from their right paw ($p<0.001$; saline-treated groups in Fig 2A) and made more left turns on day 3 after pMCAO compared to baseline ($p<0.001$; saline-treated groups in Fig. 2B). Tibia fracture alone did not affect the behavioral tests we used in the current study (Degos *et al.* 2013). Mice with pMCAO+tibia fracture took longer to remove the adhesive from the right paws ($p<0.001$; saline-treated groups in Fig. 2A), and made more left turns ($p=0.013$; Fig. 2B) than pMCAO mice on day 3 after pMCAO. These data are consistent with our previous report that tibia fracture one day after pMCAO exacerbates behavior deficit (Degos *et al.* 2013).

PHA treatment improved behavior performance in both pMCAO and pMCAO+tibia fracture groups. Compared to the saline group, PHA-treated pMCAO and pMCAO+tibia fracture mice took less time to remove the adhesive from the right paw (Fig. 2A), and made fewer left turns in the corner test (Fig. 2B). However, pMCAO+tibia fracture mice still took a longer time than pMCAO mice to remove adhesive from their right paws after PHA treatment ($p<0.001$), again indicating that tibia fracture enhanced behavior dysfunction of mice with ischemic stroke injury.

MLA treatment increased adhesive removal time (right paw) in pMCAO and pMCAO+tibia mice (Fig. 2A), and left turns in the corner test (Fig. 2B).

α-7 nAchR agonist treatment reduced infarct volume and neuronal death

Tibia fracture one day after pMCAO significantly increased the infarct volume ($p=0.005$; saline-treated groups in Fig. 3B) and TUNEL positive neurons in the peri-infarct region ($p=0.015$; saline-treated groups in Fig. 2E). These data are consistent with our previous finding that tibia fracture increases the neuronal damage of ischemic stroke (Degos *et al.* 2013). PHA reduced infarct volume (Fig. 3A & B) and TUNEL positive neurons in the peri-infarct regions (Fig. 3C, D & E) of pMCAO and pMCAO+tibia fracture mice. MLA increased infarct volume (Fig. 3A & B) and TUNEL positive neurons (Fig. 3C, D & E).

α-7 nAchR agonist treatment decreased microglia/macrophages

Compared to pMCAO mice, pMCAO+tibia fracture mice had more $CD68^+$ in the peri-infarct regions ($p=0.02$; saline-treated groups in Fig. 4C), which indicated that tibia fracture enhanced neruoinflammation during the acute stage of stroke. PHA reduced the number of $CD68^+$ cells in the peri-infarct region of pMCAO ($p<0.001$) and pMCAO+tibia fracture ($p=0.017$) mice (Fig. 4). However, pMCAO+tibia fracture mice still had more $CD68^+$ cells than pMCAO after PHA treatment ($p=0.03$), suggesting that the neuroinflammation in pMCAO+tibia fracture mice was more severe. MLA increased $CD68^+$ cells in both pMCAO and pMCAO+tibia facture mice (Fig. 4).

NIH-PA Author Manuscript

NIH-PA Author Manuscript

NIH-PA Author Manuscript

α-7 nAchR agonist treatment reduced M1 microglia/macrophages

The polarized microglia/macrophages are commonly distinguished by their expression of signature genes for surface markers and cytokines/chemokines (Hu *et al.* 2012). Using real-time PCR, we measured M1 (iNOS and CD11b) and M2 (CD206 and IL-10) marker gene expression in the infarct and peri-infarct regions. Results are presented as fold-changes relative to the mean value of saline-treated pMCAO+tibia fracture mice. pMCAO+tibia fracture mice expressed higher M1 markers than pMCAO mice: iNOS and CD11b (saline-treated groups in Fig. 5A & B). Tibia fracture did not change M2 marker, CD206 and IL-10 expression (Fig. 5C & D).

PHA reduced the expression of iNOS and CD11b (Fig. 5A & B), and increased CD206 and IL-10 (Fig. 5C & D). MLA increased the expression of iNOS and CD11b (Fig. 5A & B), and had no effect on the expression of CD206 and IL-10 (Fig. 5C & D). The expression of iNOS and CD11b was still higher in the pMCAO+tibia group compared with pMCAO-only group after PHA treatment, suggesting that with the dose we used, PHA did not completely inhibit inflammation induced by tibia fracture.

It is known that some of the M1 and M2 signature genes are expressed not only in microglia/macrophages but also in other cells in the brain. The results of real-time PCR, therefore, reflect the changes of these genes in brain tissues of mixed cell types. To evaluate whether the changes of gene expression had any indication of microglia/macrophages polarization after pMCAO or pMCAO+tibia fracture, representative M1 (CD11b)-associated or M2 (CD206)-associated marker proteins were analyzed using double immunofluorescent staining with the microglia/macrophage marker Iba1 on the peri-infarct region (Figure 6). Consistent with the real-time PCR results, tibia fracture significantly increased M1 microglia/macrophages of pMCAO mice (saline-treated group in Fig. 6B), but had no influence on the number of M2 microglia/macrophages (saline-treated group in Fig. 6D).

Compared to saline, PHA reduced M1 and MLA increased M1 microglia/macrophages (Fig. 6A & B). PHA also increased M2 cells (Fig. 6C & D), whereas MLA did not change the number of M2 cells. The M1/M2 ratio decreased after PHA treatment and increased after MLA treatment (Fig. 6E).

Because it is difficult to identify the infarct border on the surface of the brain, we collected tissue from a slightly larger area than that used in the histological analysis in order to cover the variations of infarct size and location. Since majority of $CD68^{+}$ cells were located right outside the infarct border (Figure 4B) and few were detected in the infarct region, and although the tissues in the infarct core were included in the PCR analysis, we believed that both PCR and histological analyses would measure the same M1/M2 response.

α-7 nAchR agonist treatment increased anti-oxidant gene expression and reduced NADPH oxidase and NF-κb phosphorylation

To test whether α-7 nAchR agonist reduces oxidative stress, we analyzed the expression of anti-oxidant genes, superoxide dismutase 1 (SOD1) and glutathione peroxidase 1 (GPX1), and the expression of the 2 subunits of pro-oxidative stress protein NADPH oxidase ($gp91^{phox}$ and $p22^{phox}$), using quantitative RT-PCR. NF-κb activity was analyzed by

NIH-PA Author Manuscript

NIH-PA Author Manuscript

NIH-PA Author Manuscript

quantifying phospho-NF-κb p65 positive microglia/macrophages in the peri-infarct region of pMCAO and pMCAO+tibia fracture mice, using phospho-NF-κb p65 and Iba1 antibody-stained sections. Tibia fracture reduced the expression of SOD1 and GPX1, and increased the expression of $gp91^{phox}$ and $p22^{phox}$ (Fig. 7A-D). PHA increased the expression of SOD1 (Fig. 7A) and GPX1 (Fig. 7B), and decreased the expression of $gp91^{phox}$ (Fig. 7C) and $p22^{phox}$ (Fig. 7D). MLA decreased the expression of SOD1 (Fig. 7A) and GPX1 (Fig. 7B), and increased the expression of $gp91^{phox}$ (Fig. 7C) and $p22^{phox}$ (p=0.006, Fig. 7D).

pMCAO+tibial fracture mice had more phospho-NF-κb p65 positive microglia/macrophages and phospho-NF-κb p65 in the nuclei compared to pMCAO mice (Fig. 7F). Phospho-NF-κb p65 positive microglia/macrophages and phospho-NF-κb p65 in the nuclei decreased in the PHA-treated mice (Fig. 7E & F), and increased in the MLA group (Fig. 7E & F). Thus, activation of α-7 nAchR reduced the expression of NADPH oxidase and NF-κb activity, and increased the expression of anti-oxidant genes.

Discussion

In this study, we examined the effects of PHA, the α-7 nAchR agonist, on neuroinflammation and neuronal injury in mice with contemporaneous ischemic stroke and bone fracture. We found that administration of PHA 1 and 2 days after pMCAO reduced neuronal injury and improved functional recovery. Interestingly, PHA increased anti-oxidant gene expression and reduced microglia/macrophage-infiltration, M1/M2 microglia/macrophage ratio, pro-oxidative NADPH oxidase and NF-κb activity (Table 1). These data suggest that reduction of neuroinflammation and oxidative stress might be one of the underlying mechanisms of α-7 nAchR neuroprotective effect.

We previously demonstrated that tibia fracture 1 day after ischemic stroke exacerbates neuroinflammation and injury. Blocking high-mobility-group box chromosomal protein-1 (HMGB1) using an HMGB1 antibody or depletion of macrophage with clodrolip attenuated the effects of bone fracture on stroke recovery (Degos *et al.* 2013). In this study, we found that tibia fracture increased the ratio of M1/M2 microglia/macrophages, NADPH oxidase and NF-κb activity, and reduced anti-oxidant gene expression. We also showed that the α-7 nAchR agonist, PHA, attenuates neuronal injury and behavioral dysfunction in mice with ischemic stroke only and ischemic stroke plus tibia fracture.

In addition, we demonstrated that the nAchR antagonist, MLA, had opposite effects to those of the agonist, PHA. MLA-treated mice had significantly more microglia/macrophages in the peri-infarct region, larger infarct size, more apoptotic neurons, and poorer behavioral recovery compared to either saline-treated controls or PHA-treated group. It has been reported that MLA impairs normal mouse behavior (Chilton *et al.* 2004). Our findings differ from the hemorrhagic stroke model in which MLA did not exacerbate behavioral dysfunction or increase brain edema (Krafft *et al.* 2012). One of the reasons is that the neuroinflammation in the hemorrhagic stroke model is more severe than in our pMCAO model, and a greater dose of MLA may be needed to precipitate its adverse effect.

NIH-PA Author Manuscript

NIH-PA Author Manuscript

NIH-PA Author Manuscript

Microglia/macrophages can be classified into two extreme phenotypes: M1 or M2. M1 mediates host defense and is pro-inflammatory, while M2 plays anti-inflammatory roles (Murray and Wynn 2011). Increased M1 microglia/macrophages could escalate tissue damage after stroke (Hu *et al.* 2012). We demonstrated that activation of α-7 nAchR by PHA decreased the M1 and M2 microglia/macrophage ratio. Because M2 macrophages play an anti-inflammatory role and have been shown to promote axon regeneration in culture (Kigerl *et al.* 2009), our finding suggests that the decreased M1/M2 ratio contributed to reduced ischemic injury in our model.

A previous study using a transient MCAO mouse model showed that M2 macrophages at the early stage of stroke were eventually replaced by M1 cells (Hu *et al.* 2012); the macrophage outcome in our stroke and bone fracture model is unknown. However, our results showed that tibia fracture increased M1 in the peri-infarct region without affecting M2 microglia/macrophages, suggesting that bone fracture increases neuroinflammation by promoting M1 macrophage infiltration or polarization. This needs verification through the use of transgenic mice expressing marker genes in different sub-types of microglia/macrophage, such as IL-12/23p40 (for M1) (Reinhardt *et al.* 2006), YARG (for M2) (Reese *et al.* 2007), and Ccr2-RFP^{+}/Cx3cr1GFP^{+} (for distinguishing microglia and macrophages) (Saederup *et al.* 2010).

We showed that PHA inhibits NF-κb phosphorylation, consistent with our previous finding that PHA treatment prevents TNFα-induced NF-κb activation in the hippocampi of tibia fracture mice (Terrando *et al.* 2011). In a hemorrhagic stroke model, Krafft et al demonstrated that PHA confers neuroprotection by reducing the expression of pro-apoptotic GSK-3β and activation of PI3K-Akt pathway (Krafft *et al.* 2012). PI3K-Akt has also been shown to inhibit NF-κb signaling (Guha and Mackman 2002). Therefore, decreased phospho-NF-κb p65 after PHA in our model may act through the PI3K-Akt pathway as well.

α-7 nAchR modulates vascular tones of cerebral arteries (Si and Lee 2002), but because it is difficult to monitor α-7 nAchR agonist/antagonist in awakened mice, we were not able to measure its effect on cerebral blood flow. Anesthesia could influence hemodynamic measurement and additional surgery procedure could cause additional inflammatory response, which would have complicated our analysis.

In summary, using a mouse model of pMCAO and tibia fracture, we showed that α-7 nAchR agonist treatment decreases peri-infarct microglia/macrophage infiltration, shifts microglia/macrophage polarization from M1 to M2, and downregulates NF-κb activity and oxidative gene expression, which are associated with reduction of neuronal injury and behavior deficits. Our data indicate that in addition to a previously recognized pro-survival effect, α-7 nAchR agonist also acts through downregulation of neuroinflammation and oxidative stress. Although our study could not determine if PHA's beneficial effects are secondary to the inhibition of stroke or bone-induced neuroinflammation, the fact that PHA reduces the overall neuronal injury and functional deficits in treated mice indicates that activation of α-7 nAchR could be a therapeutic opportunity for improving the outcomes of patients with stroke and bone fracture.

NIH-PA Author Manuscript

NIH-PA Author Manuscript

NIH-PA Author Manuscript

Acknowledgments

This study was supported by NIH grants P01 NS044155, R21 NS070153, R01 NS027713 and R01 GM104194. We would also like to acknowledge the support provided by the Fondation des Gueules Cassées, Paris, France. The authors thank Voltaire Gungab for manuscript preparation, and members of the UCSF Brain Arteriovenous Malformation (BAVM) Project (http://avm.ucsf.edu) for their support.

References

Anrather J, Racchumi G, Iadecola C. NF-kappaB regulates phagocytic NADPH oxidase by inducing the expression of gp91phox. J Biol Chem. 2006; 281:5657–5667. [PubMed: 16407283]

Bouet V, Freret T, Toutain J, Divoux D, Boulouard M, Schumann-Bard P. Sensorimotor and cognitive deficits after transient middle cerebral artery occlusion in the mouse. Exp Neurol. 2007; 203:555–567. [PubMed: 17067578]

Breese CR, Adams C, Logel J, et al. Comparison of the regional expression of nicotinic acetylcholine receptor alpha7 mRNA and [125I]-alpha-bungarotoxin binding in human postmortem brain. J Comp Neurol. 1997; 387:385–398. [PubMed: 9335422]

Chen H, Kim GS, Okami N, Narasimhan P, Chan PH. NADPH oxidase is involved in post-ischemic brain inflammation. Neurobiol Dis. 2011; 42:341–348. [PubMed: 21303700]

Chilton M, Mastropaolo J, Rosse RB, Bellack AS, Deutsch SI. Behavioral consequences of methyllycaconitine in mice: a model of alpha7 nicotinic acetylcholine receptor deficiency. Life Sci. 2004; 74:3133–3139. [PubMed: 15081578]

Cibelli M, Fidalgo AR, Terrando N, et al. Role of interleukin-1beta in postoperative cognitive dysfunction. Ann Neurol. 2010; 68:360–368. [PubMed: 20818791]

Degos V, Maze M, Vacas S, et al. Bone fracture exacerbates murine ischemic cerebral injury. Anesthesiology. 2013; 118:1362–1372. [PubMed: 23438676]

Durafourt BA, Moore CS, Zammit DA, Johnson TA, Zaguia F, Guiot MC, Bar-Or A, Antel JP. Comparison of polarization properties of human adult microglia and blood-derived macrophages. Glia. 2012; 60:717–727. [PubMed: 22290798]

Duris K, Manaenko A, Suzuki H, Rolland WB, Krafft PR, Zhang JH. alpha7 nicotinic acetylcholine receptor agonist PNU-282987 attenuates early brain injury in a perforation model of subarachnoid hemorrhage in rats. Stroke. 2011; 42:3530–3536. [PubMed: 21960575]

Fujii H, Hosomi N, Matsumoto M. Smoking and neurological disorders. Nihon Rinsho. 2013; 71:423–429. [PubMed: 23631229]

Go AS, Mozaffarian D, Roger VL, et al. Heart disease and stroke statistics--2013 update: a report from the American Heart Association. Circulation. 2013; 127:e6–e245. [PubMed: 23239837]

Gonzalez CL, Gharbawie OA, Kolb B. Chronic low-dose administration of nicotine facilitates recovery and synaptic change after focal ischemia in rats. Neuropharmacology. 2006; 50:777–787. [PubMed: 16469338]

Guha M, Mackman N. The phosphatidylinositol 3-kinase-Akt pathway limits lipopolysaccharide activation of signaling pathways and expression of inflammatory mediators in human monocytic cells. J Biol Chem. 2002; 277:32124–32132. [PubMed: 12052830]

Hawkins BT, Brown RC, Davis TP. Smoking and ischemic stroke: a role for nicotine? Trends Pharmacol Sci. 2002; 23:78–82. [PubMed: 11830264]

Hayakawa K, Qiu J, Lo EH. Biphasic actions of HMGB1 signaling in inflammation and recovery after stroke. Ann N Y Acad Sci. 2010; 1207:50–57. [PubMed: 20955426]

Hu X, Li P, Guo Y, Wang H, Leak RK, Chen S, Gao Y, Chen J. Microglia/Macrophage polarization dynamics reveal novel mechanism of injury expansion after focal cerebral ischemia. Stroke. 2012; 43:3063–3070. [PubMed: 22933588]

Kanis J, Oden A, Johnell O. Acute and long-term increase in fracture risk after hospitalization for stroke. Stroke. 2001; 32:702–706. [PubMed: 11239190]

Kigerl KA, Gensel JC, Ankeny DP, Alexander JK, Donnelly DJ, Popovich PG. Identification of two distinct macrophage subsets with divergent effects causing either neurotoxicity or regeneration in the injured mouse spinal cord. J Neurosci Meth. 2009; 29:13435–13444.

NIH-PA Author Manuscript NIH-PA Author Manuscript NIH-PA Author Manuscript

Klein JA, Ackerman SL. Oxidative stress, cell cycle, and neurodegeneration. J Clin Invest. 2003; 111:785–793. [PubMed: 12639981]

Krafft PR, Altay O, Rolland WB, Duris K, Lekic T, Tang J, Zhang JH. alpha7 nicotinic acetylcholine receptor agonism confers neuroprotection through GSK-3beta inhibition in a mouse model of intracerebral hemorrhage. Stroke. 2012; 43:844–850. [PubMed: 22207510]

Mazzone P, Tierney W, Hossain M, Puvenna V, Janigro D, Cucullo L. Pathophysiological impact of cigarette smoke exposure on the cerebrovascular system with a focus on the blood-brain barrier: expanding the awareness of smoking toxicity in an underappreciated area. Int J Environ Res Public Health. 2010; 7:4111–4126. [PubMed: 21317997]

Murray PJ, Wynn TA. Protective and pathogenic functions of macrophage subsets. Nat Rev Immunol. 2011; 11:723–737. [PubMed: 21997792]

Naik P, Fofaria N, Prasad S, Sajja RK, Weksler B, Couraud PO, Romero IA, Cucullo L. Oxidative and pro-inflammatory impact of regular and denicotinized cigarettes on blood brain barrier endothelial cells: is smoking reduced or nicotine-free products really safe? BMC Neurosci. 2014; 15:51. [PubMed: 24755281]

Paravicini TM, Sobey CG. Cerebral vascular effects of reactive oxygen species: recent evidence for a role of NADPH-oxidase. Clin Exp Pharmacol Physiol. 2003; 30:855–859. [PubMed: 14678250]

Quik M, Huang LZ, Parameswaran N, Bordia T, Campos C, Perez XA. Multiple roles for nicotine in Parkinson's disease. Biochem Pharmacol. 2009; 78:677–685. [PubMed: 19433069]

Raval AP, Borges-Garcia R, Diaz F, Sick TJ, Bramlett H. Oral contraceptives and nicotine synergistically exacerbate cerebral ischemic injury in the female brain. Transl Stroke Res. 2013; 4:402–412. [PubMed: 24323338]

Reese TA, Liang HE, Tager AM, Luster AD, Van Rooijen N, Voehringer D, Locksley RM. Chitin induces accumulation in tissue of innate immune cells associated with allergy. Nature. 2007; 447:92–96. [PubMed: 17450126]

Reinhardt RL, Hong S, Kang SJ, Wang ZE, Locksley RM. Visualization of IL-12/23p40 in vivo reveals immunostimulatory dendritic cell migrants that promote Th1 differentiation. J Immunol. 2006; 177:1618–1627. [PubMed: 16849470]

Saederup N, Cardona AE, Croft K, Mizutani M, Cotleur AC, Tsou CL, Ransohoff RM, Charo IF. Selective chemokine receptor usage by central nervous system myeloid cells in CCR2-red fluorescent protein knock-in mice. PLoS One. 2010; 5:e13693. [PubMed: 21060874]

Schroeter M, Jander S, Witte OW, Stoll G. Local immune responses in the rat cerebral cortex after middle cerebral artery occlusion. J Neuroimmunol. 1994; 55:195–203. [PubMed: 7530260]

Si ML, Lee TJ. Alpha7-nicotinic acetylcholine receptors on cerebral perivascular sympathetic nerves mediate choline-induced nitrergic neurogenic vasodilation. Circ Res. 2002; 91:62–69. [PubMed: 12114323]

Sun F, Jin K, Uteshev VV. A type-II positive allosteric modulator of alpha7 nAChRs reduces brain injury and improves neurological function after focal cerebral ischemia in rats. PloS One. 2013; 8:e73581. [PubMed: 23951360]

Terrando N, Eriksson LI, Ryu JK, et al. Resolving postoperative neuroinflammation and cognitive decline. Ann Neurol. 2011; 70:986–995. [PubMed: 22190370]

Tracey KJ. Reflex control of immunity. Nat Rev Immunol. 2009; 9:418–428. [PubMed: 19461672]

Tureyen K, Vemuganti R, Sailor KA, Dempsey RJ. Infarct volume quantification in mouse focal cerebral ischemia: a comparison of triphenyltetrazolium chloride and cresyl violet staining techniques. J Neurosci Methods. 2004; 139:203–207. [PubMed: 15488233]

Wang H, Yu M, Ochani M, et al. Nicotinic acetylcholine receptor alpha7 subunit is an essential regulator of inflammation. Nature. 2003; 421:384–388. [PubMed: 12508119]

Wang Z, Wei X, Liu K, et al. NOX2 deficiency ameliorates cerebral injury through reduction of complexin II-mediated glutamate excitotoxicity in experimental stroke. Free Radic Biol Med. 2013; 65:942–951. [PubMed: 23982049]

Woodruff TM, Thundyil J, Tang SC, Sobey CG, Taylor SM, Arumugam TV. Pathophysiology, treatment, and animal and cellular models of human ischemic stroke. Mol Neurodegener. 2011; 6:11. [PubMed: 21266064]

NIH-PA Author Manuscript

NIH-PA Author Manuscript

NIH-PA Author Manuscript

Yang JT, Chang CN, Wu JH, Chung CY, Weng HH, Cheng WC, Lee TH. Cigarette smoking decreases neurotrophin-3 expression in rat hippocampus after transient forebrain ischemia. Neurosci Res. 2008; 60:431–438. [PubMed: 18289710]

Zhang L, Schallert T, Zhang ZG, Jiang Q, Arniego P, Li Q, Lu M, Chopp M. A test for detecting long-term sensorimotor dysfunction in the mouse after focal cerebral ischemia. J Neurosci Methods. 2002; 117:207–214. [PubMed: 12100987]

Abbreviations

α-7 nAchR	alpha-7 nicotinic acetylcholine receptor
PHA	PHA 568487
MLA	methyllycaconitine

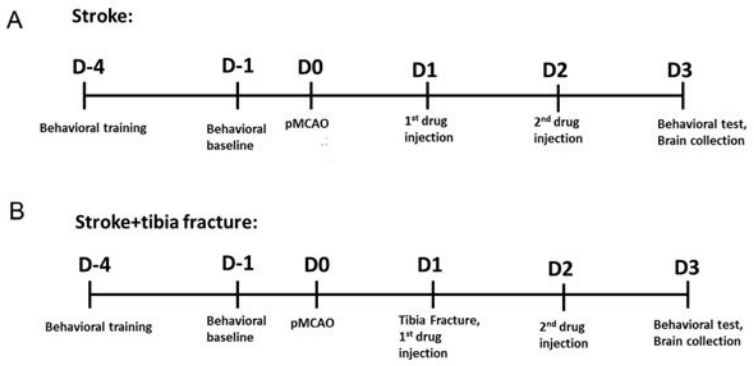

Fig. 1. Experimental design

(A) Time course for pMCAO control. *(B)* Time course for the pMCAO+tibia fracture group. All mice underwent behavioral training 4 days before pMCAO. Baseline behavior performance was documented 1 day before pMCAO (D1) and behavioral tests were performed 3 days (D3) after pMCAO. Tibial fracture was conducted 1 day (D1) after pMCAO. Drugs were injected i.p. 1 (1^{st} injection) and 2 days (2^{nd} injection) after pMCAO. Brain samples were collected after the behavior tests 3 days after pMCAO.

NIH-PA Author Manuscript NIH-PA Author Manuscript NIH-PA Author Manuscript

NIH-PA Author Manuscript

NIH-PA Author Manuscript

NIH-PA Author Manuscript

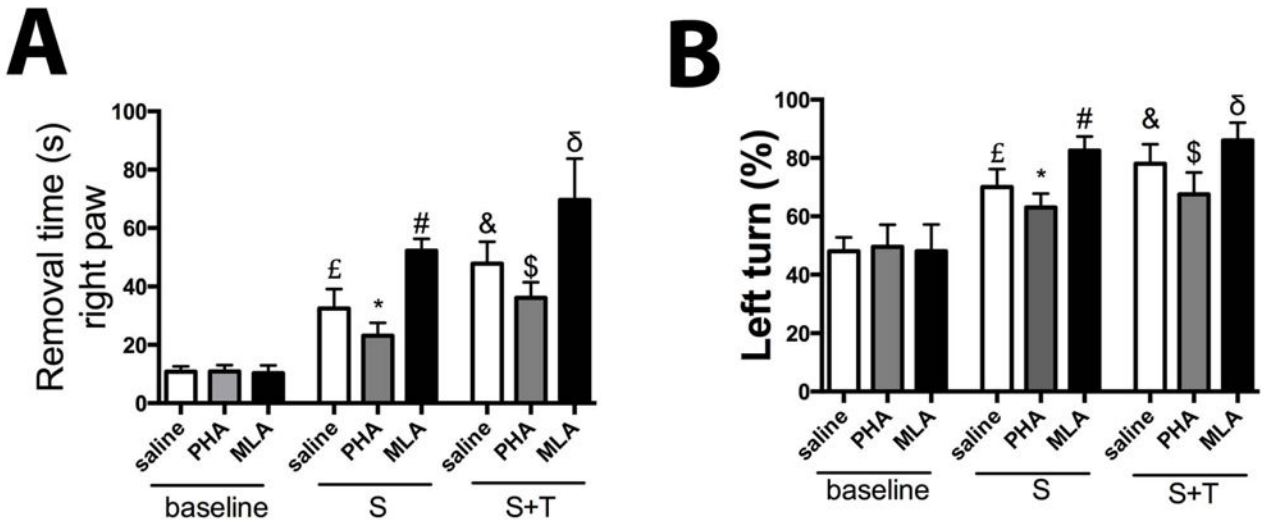

Fig. 2. α-7 nAchR agonist treatment reduced behavioral deficits

(A) Adhesive removal test (right paw). £: $p<0.001$ vs baseline; *: $p=0.005$, # $p<0.001$ and &: $p<0.001$ vs. saline-treated pMCAO (S) only mice; $: $p<0.001$ and δ: p:<0.001 vs saline-treated pMCAO+tibia fracture (S+T) mice.

(B) Corner test. £: $p<0.001$ vs saline-treated at baseline; *: $p=0.012$, # $p<0.001$ and &: $p=0.013$ vs saline-treated pMCAO mice; $: $p=0.004$ and δ: $p=0.013$ vs saline-treated pMCAO+tibia fracture mice.

NIH-PA Author Manuscript

NIH-PA Author Manuscript

NIH-PA Author Manuscript

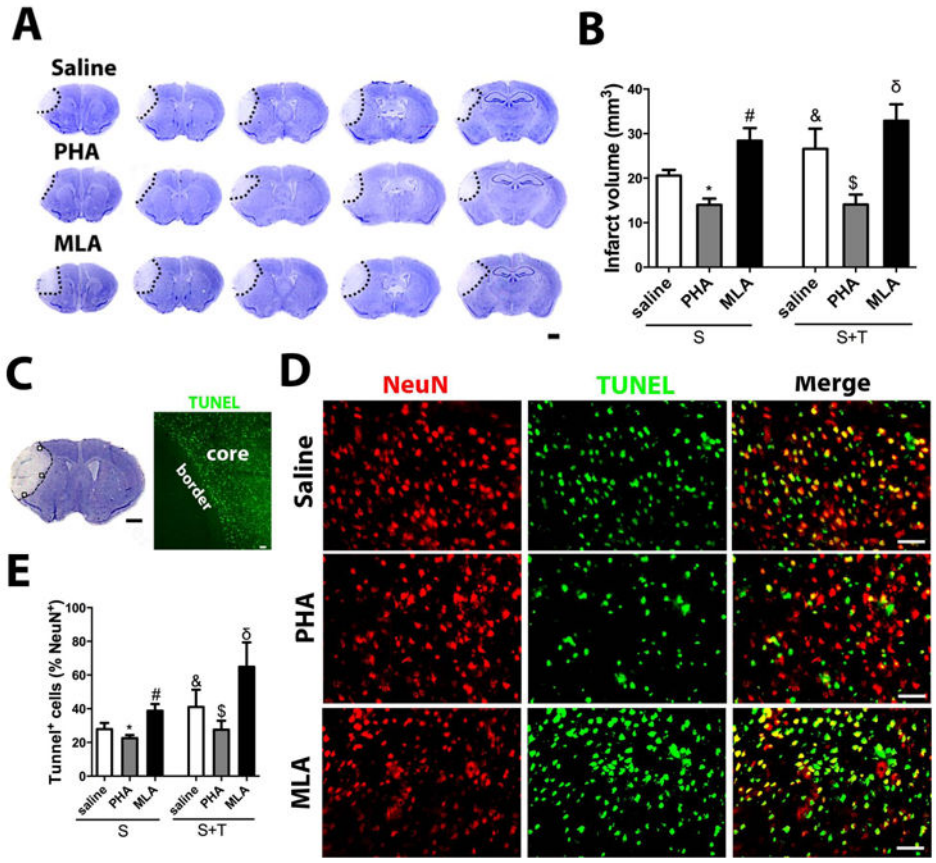

Fig. 3. α-7 nAchR agonist treatment reduced infarct volume and apoptotic neurons

(A) Representative images of cresyl violet-stained brain sections of pMCAO+tibia fracture mice. Scale bar: 1mm.

(B) Quantification of infarct volume. S: pMCAO mice; S+T: pMCAO+tibia fracture mice. *: p<0.001, # p<0.001 and &: p=0.005 vs saline-treated pMCAO only mice; $: p<0.001 and δ: p=0.015 vs saline-treated pMCAO+tibia fracture mice. *(C)* Representative images of cresyl violet-stained brain sections (bregma 1.3mm, left, scale bar: 1mm) and TUNEL-stained section(scale bar: 50um). Squares in the cresyl violet-stained section are the three regions used to quantify $NeuN^+/TUNEL^+$ cells. TUNEL-stained section shows the infarct border.

(D) Representative images of TUNEL and NeuN antibody-stained sections pMCAO+tibia fracture mice in the peri-infarct regions. Scale bar: 50um.

(E) Quantification of TUNEL positive neurons. *: p=0.01, # p<0.001 and &: p=0.015 vs. saline-treated pMCAO only mice; $: p=0.017 and δ: p=0.008 vs saline-treated pMCAO +tibia fracture mice.

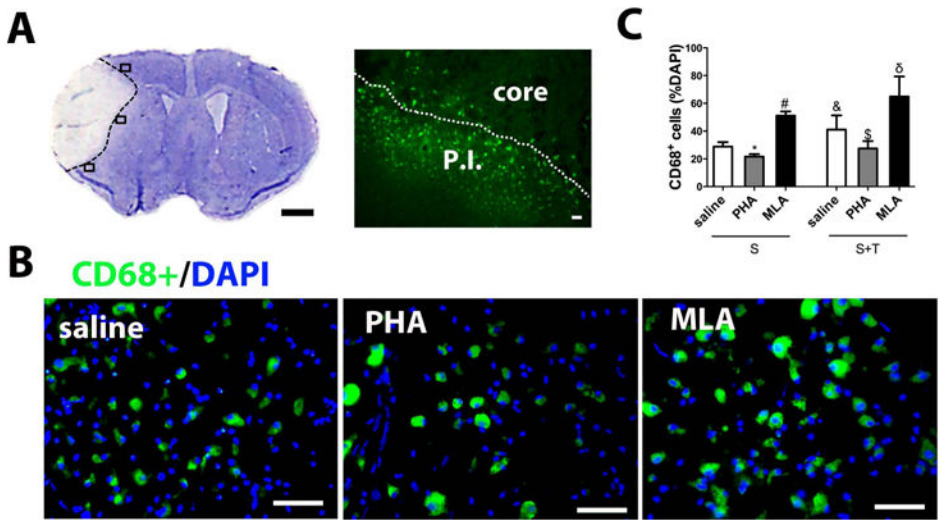

Fig. 4. α-7 nAchR agonist treatment decreased microglia/macrophages in the peri-infarct region

(A) Infarct and infarct border shown in cresyl violet-stained section (left) and CD68 antibody-stained section (right). Squares in cresyl violet-stained section were used for cell-quantification. Black (left) and white (right) dotted lines delineate the infarct border. P.I.: Peri-infarct region; Core: infarct core. Scale bars: 1 mm (left); 50 μm (right).

(B) Representative images of anti-CD68 antibody-stained sections of pMCAO+tibia fracture mice. Nuclei were counterstained with 4′,6-diamidino-2-phenylindole (DAPI). Scale bars: 50 μm.

(C) Quantification of $CD68^+$ cells. *: $p<0.001$, # $p<0.001$ and &: $p=0.02$ vs saline-treated pMCAO only mice, $: $p=0.017$ and δ: $p=0.008$ vs saline-treated pMCAO+tibia fracture mice.

S: pMCAO; T: tibia fracture.

NIH-PA Author Manuscript NIH-PA Author Manuscript NIH-PA Author Manuscript

NIH-PA Author Manuscript

NIH-PA Author Manuscript

NIH-PA Author Manuscript

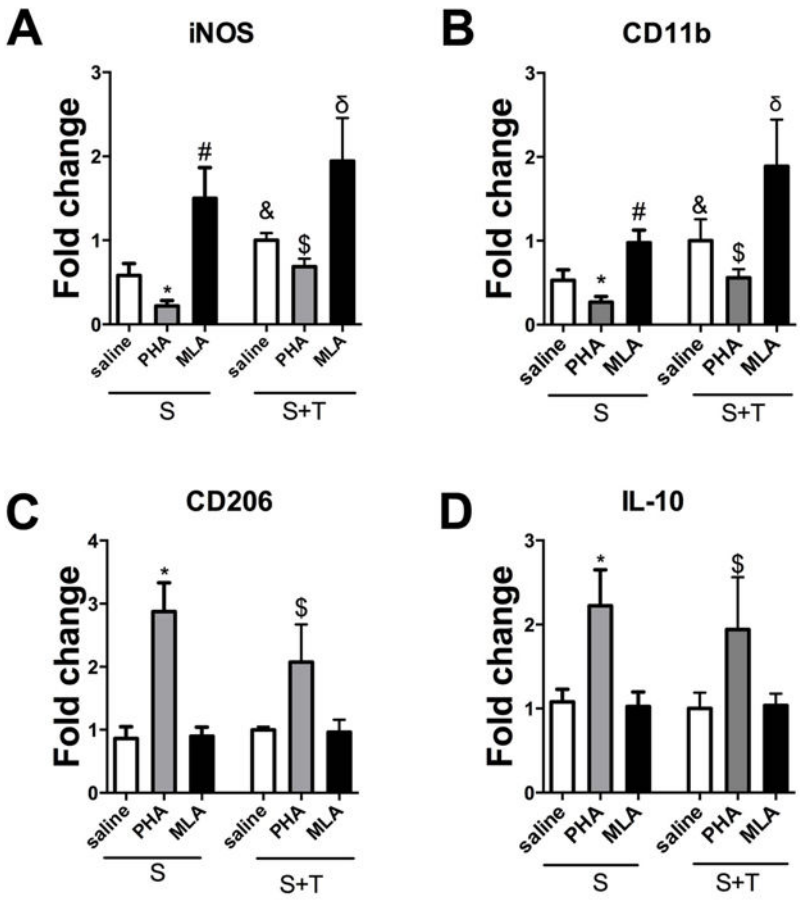

Fig. 5. α-7 nAchR agonist treatment reduced M1 and increased M2 marker gene expression

(A) Quantification of iNOS. *: p=0.004, # p=0.003 and &: p=0.002 vs saline-treated pMCAO mice; $: p=0.003 and δ: p=0.011 vs saline-treated pMCAO+tibia fracture mice.

(B) Quantification of CD11b. *: p=0.01, # p=0.004 and &: p=0.016 vs saline-treated pMCAO mice; $: p=0.019 and δ: p=0.02 vs saline-treated pMCAO+tibia fracture mice.

(C) Quantification of CD206. *: p<0.001 vs saline-treated pMCAO mice; $: p=0.011 vs saline-treated pMCAO+tibia fracture mice.

(D) Quantification of IL-10. *: p=0.002 vs saline-treated pMCAO mice; $: p=0.014 vs saline-treated pMCAO+tibia fracture mice.

S: pMCAO; T: tibia fracture.

NIH-PA Author Manuscript

NIH-PA Author Manuscript

NIH-PA Author Manuscript

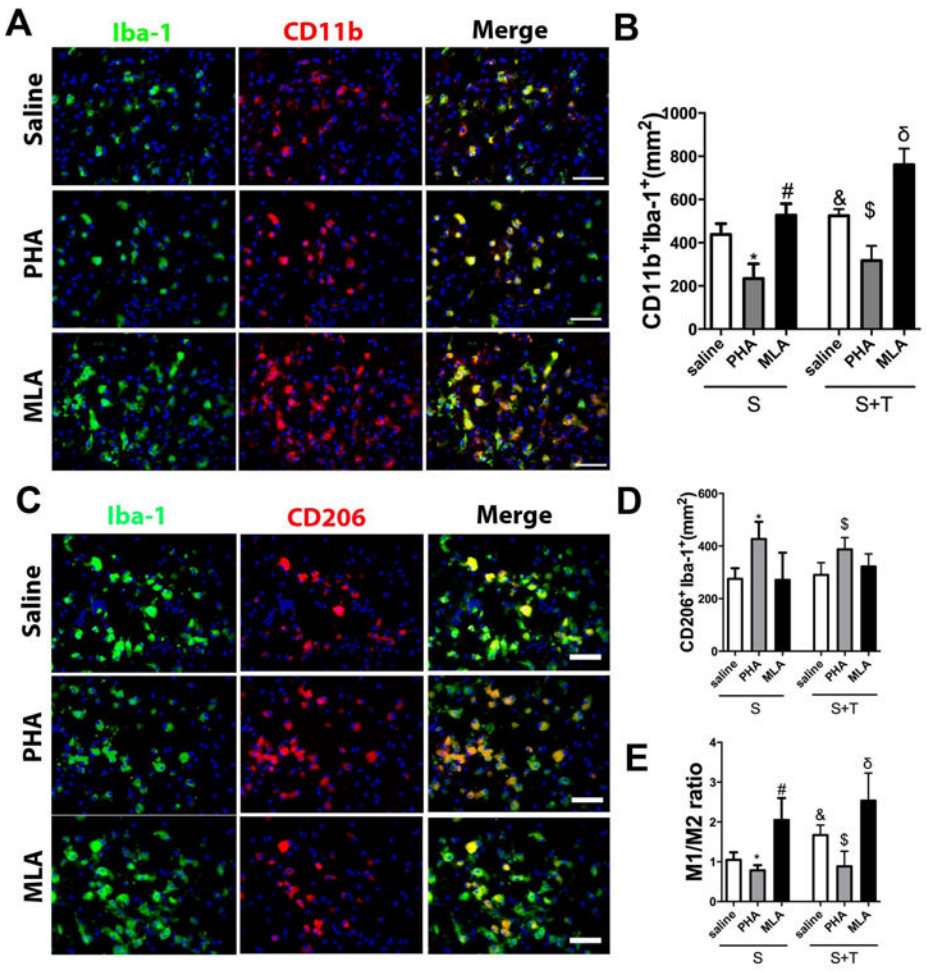

Fig. 6. α-7 nAchR agonist treatment reduced M1/M2 ratios

(A) Representative images of CD11b and Iba1 antibody-stained sections of pMCAO+tibia fracture mice. Nuclei were counterstained with DAPI. Scale bars = 50 μm.

(B) Quantification of M1 macrophages ($CD11b^+/Iba1^+$). *: $p<0.001$, # $p=0.014$ and &: $p=0.005$ vs saline-treated pMCAO only mice; $: $p=0.014$ and δ: $p=0.011$ vs saline-treated pMCAO+tibia fracture mice.

(C) Representative images of CD206 and Iba1 antibody-stained sections of pMCAO+tibia fracture mice. Nuclei were counterstained with DAPI. Scale bar= 50 μm.

(D) Quantification of M2 macrophages ($CD206^+/Iba1^+$). *: $p<0.001$, vs saline-treated pMCAO only mice; $: $p=0.001$ vs saline-treated pMCAO+tibia fracture mice.

(E) M1 to M2 ratios. *: $p=0.017$, # $p=0.002$ and &: $p=0.001$ vs saline-treated pMCAO mice; $: $p=0.003$ and δ: $p=0.017$ vs saline-treated pMCAO+tibia fracture mice.

S: pMCAO; T: tibia fracture.

NIH-PA Author Manuscript

NIH-PA Author Manuscript

NIH-PA Author Manuscript

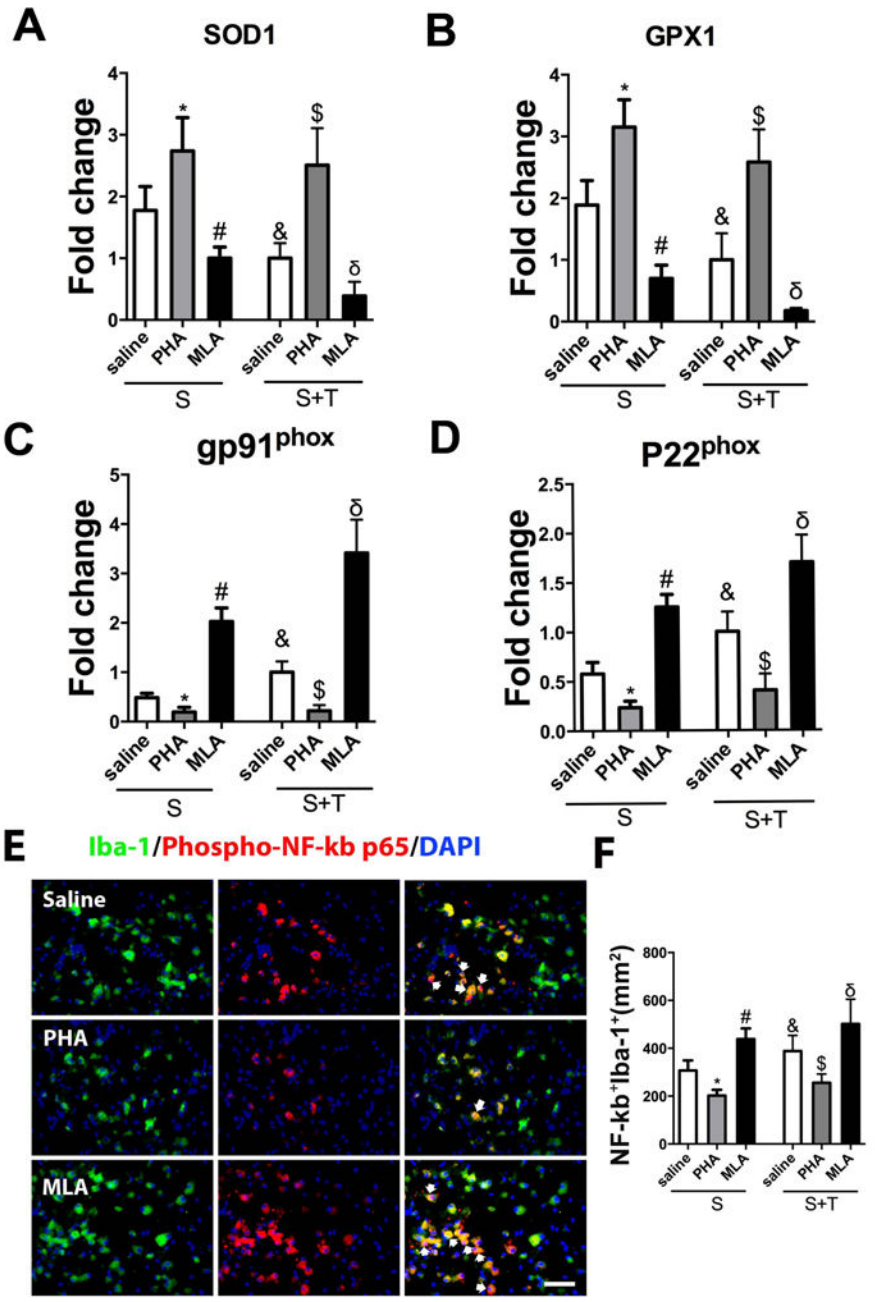

Fig. 7. α-7 nAchR agonist treatment increased anti-oxidant gene expression and reduced NADPH oxidase and NF-κb activity

(A) Quantification of SOD1. *: p=0.027, # p=0.011 and &: p=0.015 vs saline-treated pMCAO mice; $: p=0.004 and δ: p=0.011 vs saline-treated pMCAO+tibia fracture mice. *(B)* Quantification of GPX1. *: p=0.005, # p=0.002 and &: p=0.022 vs saline-treated pMCAO mice; $: p=0.003 and δ: p=0.009 vs saline-treated pMCAO+tibia fracture mice. *(C)* Quantification of $gp91^{phox}$. *: p=0.004, # p<0.001 and &: p=0.005 vs saline-treated pMCAO only mice; $: p<0.001 and δ: p<0.001 vs saline-treated pMCAO+tibia fracture mice.

(D) Quantification of $p22^{phox}$. *: p=0.002, # p<0.001 and &: p=0.011 vs saline-treated pMCAO mice; $: p=0.004 and δ: p=0.006 vs saline-treated pMCAO+tibia fracture mice.
(E) Representative images of sections obtained from pMCAO+tibia fracture mice stained with anti-phospho-NF-κb p65 and anti-Iba1 antibodies. The nuclei were counterstained with DAPI. Arrows indicate phospho-NF-κb p65 positive nuclei. Scale bar: 50 μm.
(F) Quantification of NF-$κb^+$/Iba-1^+ cells. *: p<0.001, # p<0.001 and &: p=0.016 vs saline-treated pMCAO mice; $: p<0.001 and δ: p=0.019 vs saline-treated pMCAO+tibia fracture mice.
S: pMACO; T: tibia fracture.

NIH-PA Author Manuscript
NIH-PA Author Manuscript
NIH-PA Author Manuscript

NIH-PA Author Manuscript

NIH-PA Author Manuscript

NIH-PA Author Manuscript

Table 1

Summary of the effects of PHA and MLA.

	PHA		MLA	
	S	**S+T**	**S**	**S+T**
Behavior tests	improved	improved	worsened	worsened
Infarct size	reduced	reduced	increased	increased
Apoptotic neurons	reduced	reduced	increased	increased
$CD68^+$ cells	reduced	reduced	increased	increased
M1 gene	reduced	reduced	increased	increased
M2 gene	increased	increased	unchanged	unchanged
M1 cells	reduced	reduced	increased	increased
M2 cells	increased	increased	unchanged	unchanged
M1/M2 ratio	reduced	reduced	increased	increased
Anti-oxidant gene	increased	increased	reduced	reduced
NADPH oxidase	reduced	reduced	increased	increased
NF-κb	reduced	reduced	increased	increased

S: pMCAO only; S+T: pMCAO+tibia fracture